

The Contact Percolation Transition

Tianqi Shen¹, Corey S. O'Hern^{2,1}, and M. D. Shattuck³

¹*Department of Physics, Yale University, New Haven, Connecticut 06520-8120, USA*

²*Department of Mechanical Engineering and Materials Science,
Yale University, New Haven, Connecticut 06520-8286, USA and*

³*Benjamin Levich Institute and Physics Department,
The City College of the City University of New York, New York, New York 10031, USA*

Typical quasistatic compression algorithms for generating jammed packings of athermal, purely repulsive particles begin with dilute configurations and then apply successive compressions with relaxation of the elastic energy allowed between each compression step. It is well-known that during isotropic compression athermal systems with purely repulsive interactions undergo a jamming transition at packing fraction ϕ_J from an unjammed state with zero pressure to a jammed, rigid state with nonzero pressure. Using extensive computer simulations, we show that a novel second-order-like transition, the contact percolation transition, which signals the formation of a system-spanning cluster of mutually contacting particles, occurs at $\phi_P < \phi_J$, preceding the jamming transition. By measuring the number of non-floppy modes of the dynamical matrix, and the displacement field and time-dependent pressure following compression, we find that the contact percolation transition also heralds the onset of complex spatiotemporal response to applied stress. Thus, highly heterogeneous, cooperative, and non-affine particle motion occurs in unjammed systems significantly below the jamming transition for $\phi_P < \phi < \phi_J$, not only for jammed systems with $\phi > \phi_J$.

PACS numbers: 83.80.Fg, 64.60.ah, 61.43.-j, 61.43.Gt

The jamming transition in athermal, purely repulsive particulate systems, such as granular media, foams, and colloids, has been characterized extensively in computer simulations [1] and experiments [2]. For example, when model frictionless spheres are compressed to packing fractions above ϕ_J , static particle configurations transition from unjammed to jammed with nonzero pressure (and elastic energy) and a rigid backbone of contacting particles with all positive nontrivial eigenvalues [3] of the dynamical matrix. Signatures of the jamming transition, such as anomalous scaling of the zero-frequency shear modulus with packing fraction [4] and diverging length scales [5, 6] associated with cooperative particle rearrangements, have been investigated in thermal systems [7] in the zero-temperature limit and in sheared systems [8–11] in the zero-shear rate limit, but mainly for packing fractions near and above ϕ_J .

However, there have been few detailed studies of the structural and mechanical properties of *unjammed* athermal particulate systems well below ϕ_J . As shown in Fig. 1, typical quasistatic compression algorithms used to generate static packings in experiments start with a dilute collection of particles, and the sample is successively compressed by small amounts with energy relaxation allowed between each compression step. For $\phi < \phi_J$, the configurations are not completely rigid, and thus after each small compression, particles can rearrange until all interparticle forces are zero. Despite this, the response of unjammed packings to compression and other perturbations can be highly heterogeneous, cooperative, and non-affine. Thus, an important, unanswered question is at what packing fraction does complex spatiotemporal response first occur in unjammed particulate systems?

In this letter, we describe computational studies of a

novel second-order-like transition—the contact percolation transition at ϕ_P —in athermal particulate systems of purely repulsive, frictionless disks that signals the formation of a system-spanning cluster of connected non-force-bearing interparticle contacts and the onset of complex spatiotemporal response well below the jamming transition. These systems display robust scaling behavior near ϕ_P , but with a correlation length exponent that differs from the corresponding values for random continuum [12] and rigidity percolation [13]. In addition, we find that the the number of ‘blocked’ degrees of freedom, and the particle displacement and stress relaxation time in response to compression begin to increase significantly for $\phi > \phi_P$. These results emphasize that highly cooperative and glassy dynamics occur in compressed athermal systems significantly below the jamming transition, not only for jammed systems with $\phi > \phi_J$.

We focus on systems composed of bidisperse frictionless disks that interact via the purely repulsive linear spring potential:

$$V(r_{ij}) = \frac{\epsilon}{2} \left(1 - \frac{r_{ij}}{\sigma_{ij}}\right)^2 \theta\left(1 - \frac{r_{ij}}{\sigma_{ij}}\right), \quad (1)$$

where ϵ is the characteristic energy scale, $\theta(x)$ is the Heaviside step function, r_{ij} is the separation between the centers of disks i and j , and $\sigma_{ij} = (\sigma_i + \sigma_j)/2$ is their average diameter. We chose a 50–50 (by number) mixture of large and small disks with diameter ratio $\sigma_l/\sigma_s = 1.4$ to inhibit crystallization [1] and implemented periodic boundary conditions in a unit square. We employed a quasistatic isotropic compression algorithm to generate static packings over a range of packing fractions [14]. We initialize each system with random particle positions at $\phi = 0$ and zero velocities. We then compress the sys-

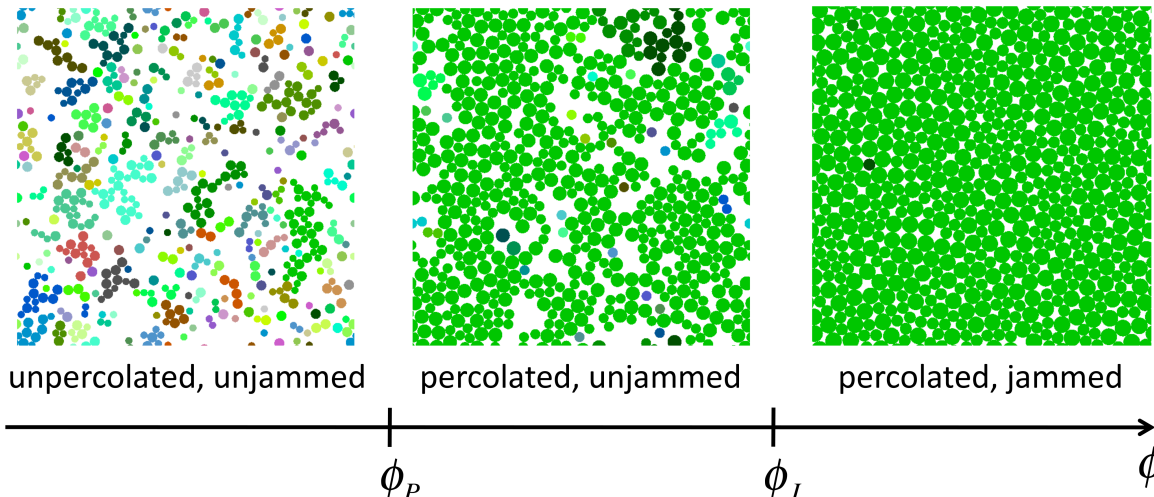


FIG. 1: (Color online) Typical snapshots from the quasistatic isotropic compression algorithm to generate static particle configurations as a function of packing fraction ϕ . Particles with a given color shading belong to the same cluster of mutually contacting particles. For (left) $\phi < \phi_P$, the system is unjammed, and the largest cluster of contacting particles does not percolate. The largest cluster begins to percolate for (middle) $\phi_P < \phi < \phi_J$, but the system remains unjammed since it possesses nontrivial floppy modes. For (right) $\phi > \phi_J$, the percolating cluster of contacting particles has become rigid except for a small number of rattlers [16], and the system is jammed.

tem in steps of $\Delta\phi = 10^{-3}$ and relax the small particle overlaps after each step by solving Newton's equations of motion in the overdamped limit,

$$m\vec{a}_i = \sum_j \vec{F}(r_{ij}) - b\vec{v}_i, \quad (2)$$

where m and \vec{a}_i are the particle mass and acceleration, $\vec{F}(r_{ij}) = -dV(r_{ij})/dr_{ij}\hat{r}_{ij}$, \hat{r}_{ij} is the unit vector connecting the centers of particles i and j , and $\tilde{b} = b\sigma_s/\sqrt{m\epsilon}$ is the damping coefficient, until the total potential energy per particle falls below a specified tolerance $V/\epsilon N < V_{\text{tol}} = 10^{-16}$. We studied two values for the damping coefficient, $\tilde{b} = 1$ and $\tilde{b} \rightarrow \infty$ using steepest descent dynamics. We continue compression steps followed by relaxation until the systems jam at a configuration dependent $\phi_J \approx 0.84$.

In Fig. 2, we characterize the contact percolation transition by plotting the probability $P(\phi)$ that the system forms a system-spanning network of interparticle contacts in either the x - or y -direction, where contact is determined by $r_{ij} \leq \sigma_{ij}$, at each ϕ immediately following a compression step. We find that the contact percolation transition at $\phi_P = 0.549 \ll \phi_J$ becomes sharper with system size and obeys finite-size scaling, but with a correlation length exponent $\nu \approx 1.68$ that is significantly larger than that for random continuum [12] and rigidity percolation [13], but smaller than that found for contact percolation in athermal particulate systems with short-range attractions [15]. (Note that percolation onset occurs at a similar value $\phi_P = 0.558 \pm 0.008$ for athermal systems with short-range attractions.) In contrast, the exponent $\tau \approx 2.01$ that characterizes the power-law scaling of the cluster size distribution and the fractal di-

mension $D \approx 1.89$ are similar to that for random continuum percolation and contact percolation for athermal systems with short-range attractions, and obey hyperscaling $D(\tau - 1) = 2$. (See Table I.) We find that these results are insensitive to the damping coefficient \tilde{b} in the overdamped limit and compression step for $\Delta\phi \leq 10^{-3}$.

We have shown that immediately following each compression step, a system-spanning cluster of interparticle contacts forms at $t = 0$ for $\phi \geq \phi_P$, much below ϕ_J . To determine if this purely geometrical transition influences the mechanical properties of the system, we measure the eigenvalues of the dynamical matrix at $t = 0$ following each compression step. As static packings are compressed, they progressively become less floppy, *i.e.* fewer single and collective particle motions cost zero energy. We quantify the increase in rigidity by measuring the fraction of non-floppy or 'blocked' eigenmodes $F(\phi)$ —the ratio of the number N_{nf} of non-zero eigenvalues of the dynamical matrix to the total number of nontrivial modes $2N' - 2$ (where $N' = N - N_r$ and N_r is the number of rattler particles at jamming [16])—over a range of packing fractions. With this definition, $F(\phi_J) = 1$. In Fig. 3 (a), we show that the fraction of non-floppy modes $F(\phi)$ grows linearly with ϕ for small ϕ and near jamming $F(\phi)$ scales as $1 - A(\phi_J - \phi)^\alpha$ with $A \approx 0.99$ and $\alpha \approx 0.6$. We find that $F(\phi)$ begins to deviate from linear behavior near ϕ_P . In addition, near ϕ_P , $F(\phi)$ does not obey the scaling behavior near ϕ_J . Thus, we have identified a signature in the mechanical response near ϕ_P .

In addition, we find that the contact percolation transition at ϕ_P signals the onset of complex spatiotemporal response to isotropic compression. We measure two quantities that characterize cooperative particle motion:

Percolation type	ν	τ	D
Repulsive contact	1.70 ± 0.09	2.01 ± 0.04	1.89 ± 0.03
Attractive contact	1.92 ± 0.03	2.04 ± 0.04	1.88 ± 0.04
Continuum	1.34 ± 0.02	2.02 ± 0.03	1.91 ± 0.04

TABLE I: Critical exponents for contact percolation in athermal systems with purely repulsive interactions and short-range attractive interactions [15], as well as random continuum percolation [12] in 2D.

1) the displacement in configuration space between systems at successive compressions,

$$D = \sqrt{\sum_{i=1}^N [(x_i(0) - x_i(\infty))^2 + (y_i(0) - y_i(\infty))^2]}, \quad (3)$$

where $(x_i(0), y_i(0))$ and $(x_i(\infty), y_i(\infty))$ are the locations of particle i at $t = 0$ and $t \rightarrow \infty$, respectively, during the energy relaxation, and 2) the accumulated distance traveled in configuration space,

$$L = \int_0^\infty dt \sqrt{\sum_{i=1}^N \dot{v}_i^2(t)} \quad (4)$$

from $t = 0$ after the compression to the end of the energy relaxation. Both D and L are normalized by the compression step size $\Delta\phi$. In Fig. 3 (b), we show that D and L grow roughly exponentially for small ϕ , but begin to deviate from the low- ϕ behavior near ϕ_P . An even larger signature of collective, non-affine motion is shown in the inset to Fig. 3 (b). The difference $L - D$ begins to increase dramatically at $\phi_l \approx 0.78$, which is also significantly below ϕ_J . Thus, for $\phi > \phi_P$ particles move collectively in response to compression, but for $\phi > \phi_l$ after relaxation they end up close to where they started.

We also characterize the time-dependent response to compression. In Fig. 4 (a), we plot the normalized pressure $\tilde{p} \equiv p(t)/p(0)$ as a function of time following a compression step $\Delta\phi = 10^{-3}$ over a wide range of packing fractions. The normalized pressure develops a plateau near $\tilde{p} = 0.6$ and decays more slowly with increasing packing fraction. The plateau in the normalized pressure suggests that significant decay of the pressure in the system requires first the collective motion of exterior particles in percolating clusters followed by motion of the interior particles. In Fig. 4 (b), we plot the pressure relaxation time t^* , *i.e.* the time at which the normalized pressure has decayed to a specified small value $\tilde{p} = 10^{-4}$. The shape of the increase in the pressure relaxation time is relatively insensitive to \tilde{b} (for overdamped dynamics) and \tilde{p} . In the inset to Fig. 4 (b), the logarithmic slope of t^* with respect to ϕ shows a subtle increase near ϕ_P , but a much more dramatic increase near ϕ_l , where the the measure of cooperative motion increased significantly. (See the inset to Fig. 3 (b).) Thus growth in the stress relaxation time occurs at packing fractions significantly below ϕ_J .

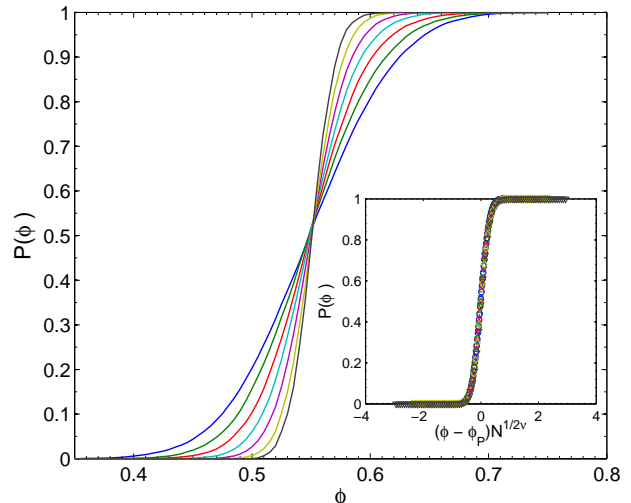


FIG. 2: Percolation probability $P(\phi)$ that the system possesses a system-spanning cluster (in either the x - or y -direction) immediately following a compression step $\Delta\phi = 10^{-3}$ versus packing fraction ϕ for $N = 10^3$ versus packing fraction ϕ for $N = 100, 200, 400, 800, 1600, 3200,$ and 6400 particles (from left to right) averaged over 400 configurations. Inset: Same as the main figure except the horizontal axis is scaled by $(\phi - \phi_P)N^{1/2\nu}$, where $\phi_P = 0.549 \pm 0.001$ and $\nu = 1.70 \pm 0.09$.

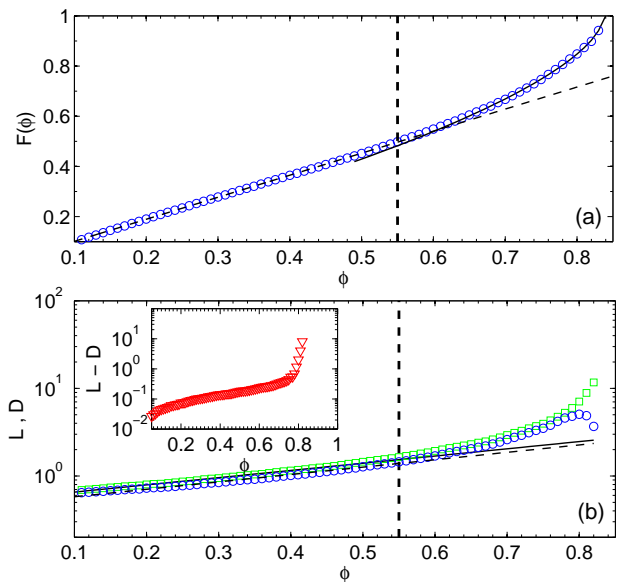


FIG. 3: (a) The fraction $F(\phi)$ of non-floppy eigenmodes of the dynamical matrix in the system measured immediately after a compression step of $\Delta\phi = 10^{-3}$ over a range of packing fractions for $N = 1000$. Fits to the low and high ϕ behavior of $F(\phi)$ are shown as dashed and solid lines, respectively. (b) The accumulated distance L and displacement D between successive compressions normalized by $\Delta\phi$ as a function of packing fraction. The low- ϕ , roughly exponential behavior of L and D is indicated by solid and dashed lines. The inset shows $L - D$ versus ϕ . In both panels, the vertical line indicates the percolation transition $\phi_P = 0.549$.

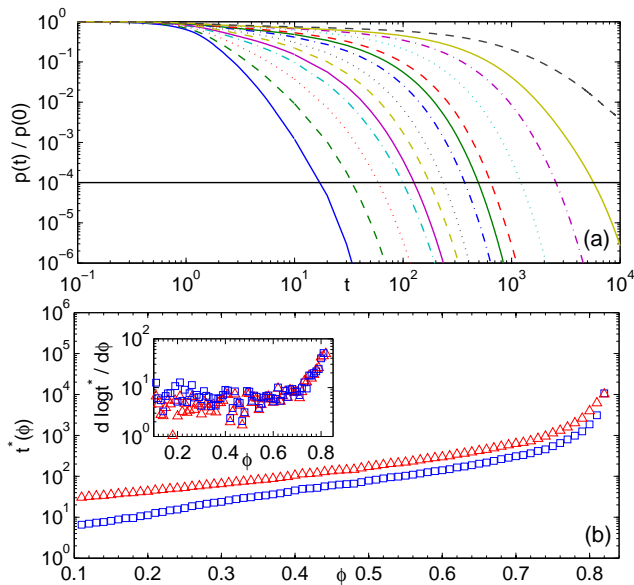


FIG. 4: (a) Normalized pressure $\tilde{p} \equiv p(t)/p(0)$ versus t following a compression step $\Delta\phi = 10^{-3}$ with $\tilde{b} = 1$ over a range of packing fractions including $\phi = 0.2, 0.3, 0.4, 0.5, 0.55, 0.6, 0.65, 0.7, 0.73, 0.75, 0.78, 0.8, 0.81,$ and 0.82 (from left to right) for $N = 200$. The horizontal line $\tilde{p} = 10^{-4}$ indicates the normalized pressure at which the pressure relaxation time t^* was measured. (b) The pressure relaxation timescale $t^*(\phi)$ for systems with $\tilde{b} \rightarrow \infty$ (triangles) and 1 (squares). The inset shows the logarithmic derivative of t^* with respect to ϕ .

In this letter, we described extensive computational studies of the geometrical and mechanical properties of unjammed, athermal particulate systems undergoing quasistatic isotropic compression. A novel aspect of

our work is that we focused on unjammed rather than jammed configurations [17]. We first showed that these systems undergo the ‘contact percolation’ transition at $\phi_P < \phi_J$, much below the jamming transition. Above ϕ_P , these systems possess a system-spanning cluster of non-force bearing interparticle contacts. Near the transition, the cluster size distribution displays robust scaling with system size with a correlation length exponent ν that is larger [15] than that for random continuum and rigidity percolation, and thus contact percolation belongs to a distinct universality class. We also performed measurements to assess the mechanical properties and time-dependent stress response for unjammed systems with $\phi_P < \phi < \phi_J$. We found three key results: 1) the increase in the fraction F of non-floppy modes begins to deviate from the low- ϕ behavior near ϕ_P and the acceleration of non-floppy modes near ϕ_P is distinct from the approach to $F = 1$ near ϕ_J . 2) The ϕ -dependence of two measures of cooperative motion—the accumulated distance L and displacement D in configuration space between successive compressions—deviates from the low- ϕ behavior near ϕ_P . Further, their difference $L - D$ begins to grow dramatically near $\phi_l \approx 0.78$, which signals blocking in configuration space well below ϕ_J . 3) The growth in the stress relaxation time t^* also begins to deviate from the low- ϕ behavior near ϕ_l . Thus, the process of rigidification and the onset of cooperative, heterogeneous, and slow dynamics occurs well below jamming onset in athermal particulate systems.

Acknowledgments This research was supported by the National Science Foundation under Grant Nos. DMS-0835742 (CO, TS), PHY-1019147 (TS), and CBET-0968013 (MS).

-
- [1] C. S. O’Hern, L. E. Silbert, A. J. Liu, and S. R. Nagel, *Phys. Rev. E* **68** (2003) 011306.
- [2] T. S. Majmudar, M. Sperl, S. Luding, and R. P. Behringer, *Phys. Rev. Lett.* **98** (2007) 058001.
- [3] A. Tanguy, J. P. Wittmer, F. Leonforte, J.-L. Barrat, *Phys. Rev. B* **66** (2002) 174205.
- [4] W. G. Ellenbroek, Z. Zeravcic, W. van Saarloos, and M. van Hecke, *Europhys. Lett.* **87** (2009) 34004.
- [5] J. A. Drocco, M. B. Hastings, C. J. Olson Reichhardt, and C. Reichhardt, *Phys. Rev. Lett.* **95** (2005) 088001.
- [6] L. E. Silbert, A. J. Liu, and S. R. Nagel, *Phys. Rev. Lett.* **95** (2005) 098301.
- [7] Z. Zhang, N. Xu, D. T. N. Chen, P. Yunker, A. M. Alsayed, K. B. Aptowicz, P. Habdas, A. J. Liu, S. R. Nagel, and A. G. Yodh, *Nature* **459** (2009) 230.
- [8] B. P. Tighe, E. Woldhuis, J. J. C. Remmers, W. van Saarloos, and M. van Hecke, *Phys. Rev. Lett.* **105** (2010) 088303.
- [9] C. Heussinger, L. Berthier, and J.-L. Barrat, *Europhys. Lett.* **90** (2010) 20005.
- [10] C. Heussinger and J.-L. Barrat, *Phys. Rev. Lett.* **102** (2009) 218303.
- [11] D. Vågberg, D. Valdez-Balderas, M. A. Moore, P. Olsson, and S. Teitel, *Phys. Rev. E* **83** (2011) 030303(R).
- [12] E. T. Gawlinski and H. G. Stanley, *J. Phys. A: Math. Gen.* **14** (1981) L291.
- [13] D. J. Jacobs and M. F. Thorpe, *Phys. Rev. Lett.* **75** (1995) 4051.
- [14] G.-J. Gao, J. Blawdziewicz, and C. S. O’Hern, *Phys. Rev. E* **74** (2006) 061304.
- [15] G. Lois, J. Blawdziewicz, and C. S. O’Hern, *Phys. Rev. Lett.* **100** (2008) 028001.
- [16] Jammed systems possess all positive nontrivial eigenvalues of the dynamical matrix except for d zero eigenvalues per rattler particle with fewer than $d + 1$ contacts, where d is the spatial dimension.
- [17] S. Ostojic, E. Somfai, and B. Nienhuis, *Nature* **439** (2006) 828.